Myocardial Perfusion Imaging

Sebastian Kozerke, PhD

Institute for Biomedical Engineering, University and ETH Zurich, Zurich, Switzerland
Imaging Sciences and Biomedical Engineering, King's College London, UK

Target audience

The lecture targets physicists, engineers and clinicians with an interest in myocardial perfusion imaging methodology and its clinical application.

Preface

Following the proof-of-concept study of contrast-enhanced myocardial perfusion imaging in isolated hearts in 1990 (1) and in cardiac patients in 1991 (2) significant advances have been made. Clinical trials have proven the diagnostic performance of the method in large patient cohorts (3,4) in comparison with invasive coronary angiography and nuclear techniques. Besides application of exogenous contrast agents, endogenous contrast mechanisms have been explored too. Arterial spin labeling in the heart was demonstrated in 1993 (5) and, with further technical improvements, recent patient studies have demonstrated the clinical value of the method (6). Nevertheless, the perfusion-induced contrast is small and hence spin labeling methods remain challenging. Accordingly, and based on the clinical data available today, this plenary lecture will focus on the state-of-the-art of contrast-enhanced myocardial perfusion imaging approaches.

Introduction

While spatial and temporal resolution, spatial coverage and robustness against motion and other artifacts are parameters of general concern in every imaging experiment, contrast-enhanced perfusion imaging additionally requires knowledge of the relationship between the signal and T_1 changes as induced by the contrast agent bolus:

$$\frac{1}{T_1} = \frac{1}{T_{10}} + \Gamma \cdot [Gd] \qquad [1]$$

Here, T_{10} and Γ denote baseline T_1 and relaxivity of the contrast agent, respectively. In principle, the T_1 dependency of driven steady-states may be exploited to derive contrast agent concentration (7); however, the transient phase to steady-state often renders the approach problematic. Accordingly, magnetization preparation schemes either using inversion or saturation pre-pulses have been widely adopted (Figure 1).

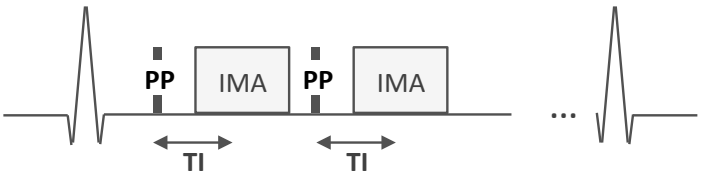

Figure 1. Perfusion sequence including pre-pulse (PP) and imaging module (IMA). The time between pre-pulse and k-space center is denoted by TI.

Saturation may be achieved by using simple hard pulses or, if B_1+ inhomogeneity is present, by composite or adiabatic pre-pulses (8). The saturation recovery method is independent of heart rate variations and hence very robust in patients. It is, however, readily seen that a linear relationship between image intensity $\rho(\vec{x})$ and contrast agent concentration is only obtained for very short delays TI between pre-pulse and imaging readout or for low contrast agent concentrations:

$$\rho(\vec{x}) \propto M_0\left(1 - e^{-TI/T_1(\vec{x})}\right) \qquad [2]$$

i.e. for $TI \ll T_1$ for which $e^{-TI/T_1} \approx 1 - TI/T1$. While a linear relationship between signal and contrast agent concentration is desirable for quantitative perfusion analysis (9), the associated low agent concentration reduces the contrast-to-noise ratio between non-ischemic and ischemic myocardium and hence may compromises qualitative reading. With contrast agent concentrations of 0.05 to 0.1 mmol/kg, as used clinically, there is already significant departure from linearity (10). In order to capture the non-linear signal/concentration relationship dedicated modifications to the pulse sequence have been proposed. In the *dual-bolus technique* (11) a diluted pre-bolus is imaged while the *dual-sequence technique* (12) interleaves a second sequence with reduced TI. From a practical point of view of contrast agent administration the dual-sequence approach is preferred (Figure 2).

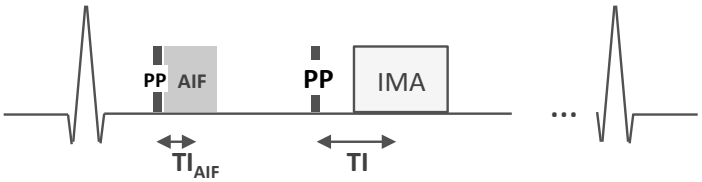

Figure 2. Dual-sequence technique including module to image the arterial input function (AIF) with a short delay between pre-pulse and k-space center followed by the standard perfusion imaging module.

Pulse sequences

On clinical systems multi-slice 2D perfusion protocols are most widely available. Three to four slices are imaged in each cardiac cycle using either gradient-echo (GRE), gradient echo-planar (GRE-EPI) or balanced steady-state free precession (bSSFP) pulse sequences (13) (Figure 3). A key disadvantage of the multi-slice 2D approach relates to the limited coverage of the heart and the fact that different slices are acquired in different phases throughout the cardiac cycle. To address the issue, 3D perfusion imaging in combination with *scan acceleration* has been developed (14) providing whole-heart coverage in a single or even in multiple cardiac phases.

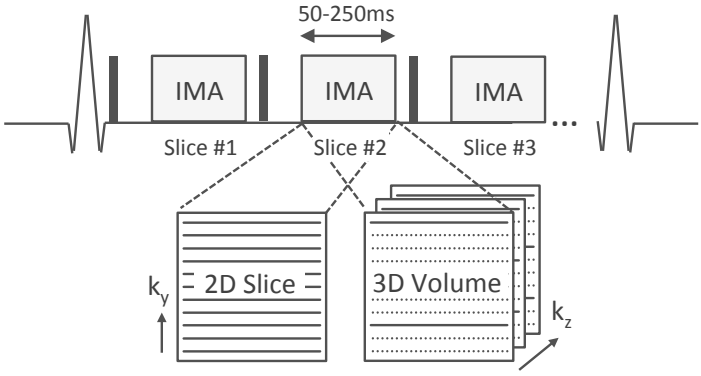

Figure 3. Multi-slice 2D versus volumetric 3D perfusion imaging. While 2D imaging is feasible within the limited acquisition window per cardiac cycle, 3D imaging approaches require data undersampling.

In general, cardiac motion demands very rapid data acquisition within a 50-250ms window per cardiac cycle. This requirement inherently limits spatial resolution and coverage that can be obtained with Fourier encoding or conventional parallel imaging techniques. For example, for a 100ms acquisition interval per cardiac cycle, a TR of 2.5ms, 75% partial Cartesian sampling and parallel imaging with 2-fold undersampling, the minimum in-plane resolution is 3mm. At this resolution, sub-endocardial perfusion defects may already be difficult to discern.

Scan acceleration

With advances in spatiotemporal undersampling methods, undersampling factors beyond a factor of two are now routinely obtained (15). The developments have triggered a range of developments including high-resolution 3D perfusion imaging (16). Spatiotemporal or k-t undersampling may be considered independent of the actual k-space

trajectory used by e.g. considering sampling pattern in angle and time space as in Radial imaging (Figure 4). As a common feature of spatiotemporal undersampling methods, the inherent similarity of adjacent points in both space and time is exploited.

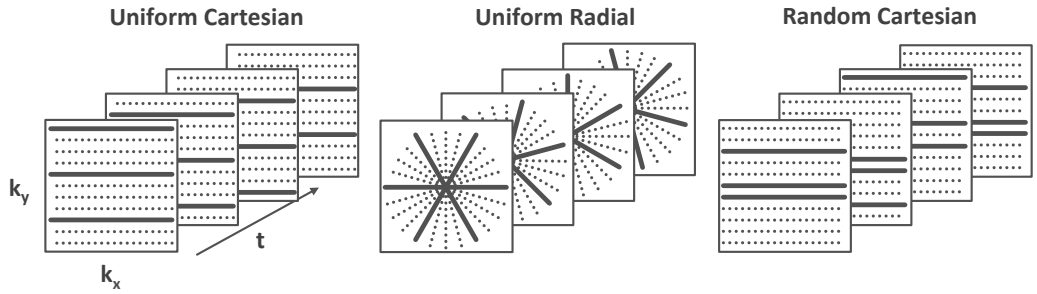

Figure 4. Temporal undersampling using k-t pattern in Cartesian and Radial sampling. Data may be collected using either uniform steps in k-t space or using random steps as required for Compressed Sensing.

In order to briefly discuss implementations of scan acceleration, let us define *MR encoding* of the discretized set of voxels $\vec{\rho}$ as:

$$\vec{d} = \Gamma \cdot FT \cdot S \cdot \vec{\rho} + \vec{n} \qquad [3]$$

with $\vec{d}$ stacking the measured k-space data for all receiver coils, Γ denoting the undersampling operator, FT the Fourier transform operator, coil sensitivities S and noise $\vec{n}$. By introducing matrix $E = \Gamma \cdot FT \cdot S$ image reconstruction or *MR decoding* may be written as:

$$\vec{\imath} \rightarrow \text{argmin}_{\text{i}} \left(\vec{d} - E \cdot \vec{\imath}\right)^{H} \psi^{-1} \left(\vec{d} - E \cdot \vec{\imath}\right) \qquad [4]$$

where ψ refers to the noise covariance matrix as determined from noise measurements and i denotes the image to be reconstructed. The inversion of [3] is ill-posed if undersampling is employed. Accordingly, an infinite number of solutions exist and hence regularization is required to solve the problem:

$$\vec{\imath} \rightarrow \text{argmin}_{\text{i}} \left\| \vec{d} - E \cdot \vec{\imath} \right\|_2^2 + \lambda \| \Theta^{-1} \cdot \vec{\imath} \|_2^2 \qquad [5]$$

Here Θ contains prior information about the object which may include an estimate of the expected signal in the spatiotemporal frequency (x-f) domain as in k-t SENSE (17) or in the space-principal component domain as in k-t PCA (18). In the context of incoherent or random undersampling , the norm of the regularizer in [5] may be modified to promote sparse solutions (19):

$$\vec{\imath} \rightarrow \text{argmin}_{\text{i}} \left\| \vec{d} - E \cdot \vec{\imath} \right\|_2^2 + \lambda \| \Phi \cdot \vec{\imath} \|_1 \qquad [6]$$

where Φ refers to an operator to transform the image estimate into a sparse representation. In a particular implementation, the sparsifying transform consists of the spatio-temporal gradient or total variation operator (20). There is a wide range of different implementations of the fundamental concepts available today.

Clinical application

Example images of contrast-enhanced 3D perfusion images acquired with 10x k-t PCA in a cardiac patient are demonstrated in Figure 5. Based on the whole-heart coverage of the method, image fusion of 3D perfusion maps with low-dose CT angiographic data becomes possible (21).

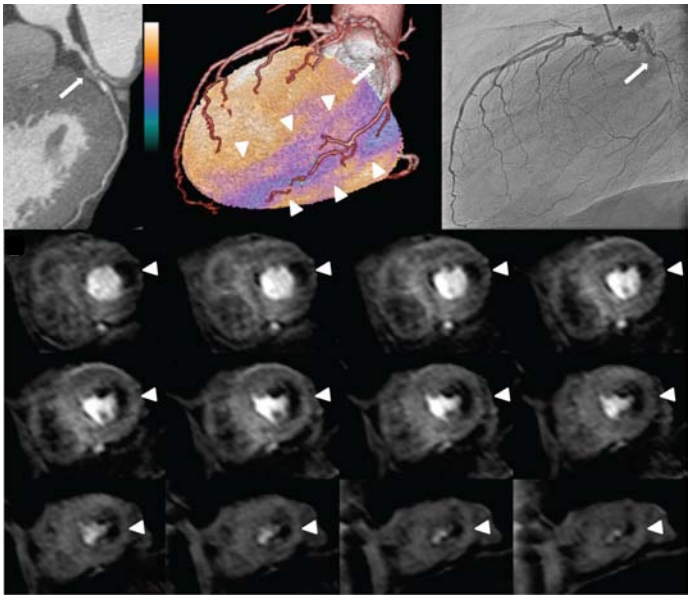

Figure 5. 3D myocardial perfusion images (lower panel) revealing a lateral perfusion defect in a 65-year old patient. The perfusion defect and the culprit lesion are seen matched in the image fusion of MR perfusion and CT angiography data (top panel, center); adapted from (21).

Meanwhile a number of clinical studies using highly accelerated 2D and 3D perfusion imaging methodology have been published (22-25) providing data on the benefit of high spatial resolution and/or whole-heart coverage. Based on current evidence, the translation of the methods for wider use is warranted.

Outlook

Further technical advances are under way to push spatiotemporal resolution by exploiting compressed sensing and parallel imaging jointly (26), by radial and spiral trajectories in conjunction with k-t undersampling (27,28) or by using localized spatio-temporal constraints (29). A very interesting avenue of development concerns new approaches for driven steady-state imaging without magnetization preparation or gating (30,31) simplifying the patient setup and increasing robustness against arrhythmias.

While most clinical studies so far have used qualitative or semi-quantitative perfusion metrics, absolute quantification of myocardial blood flow is much desired (32). The impact of scan acceleration, noise and other artifacts on quantitative analysis is a current topic of research and will be briefly discussed.

References

1. Atkinson DJ, Burstein D, Edelman RR. First-Pass Cardiac Perfusion: Evaluation With Ultrafast MR Imaging. Radiology 1990;174:757–762.

2. Manning WJ, Atkinson DJ, Grossman W, Paulin S, Edelman RR. First-pass nuclear magnetic resonance imaging studies using gadolinium-DTPA in patients with coronary artery disease. Journal of the American College of Cardiology 1991;18:959–965. doi: 10.1016/0735-1097(91)90754-W.

3. Schwitter J, Wacker CM, van Rossum AC, et al. MR-IMPACT: comparison of perfusion-cardiac magnetic resonance with single-photon emission computed tomography for the detection of coronary artery disease in a multicentre, multivendor, randomized trial. European Heart Journal 2008;29:480–489. doi: 10.1093/eurheartj/ehm617.

4. Greenwood JP, Maredia N, Younger JF, et al. Cardiovascular magnetic resonance and single-photon emission computed tomography for diagnosis of coronary heart disease (CE-MARC): a prospective trial. Lancet 2012;379:453–460. doi: 10.1016/S0140-6736(11)61335-4.

5. Williams DS, Grandis DJ, Zhang W, Koretsky AP. Magnetic resonance imaging of perfusion in the isolated rat heart using spin inversion of arterial water. Magn Reson Med 1993;30:361–365. doi: 10.1002/mrm.1910300314.

6. Zun Z, Varadarajan P, Pai RG, Wong EC, Nayak KS. Arterial spin labeled CMR detects clinically relevant increase in myocardial blood flow with vasodilation. JACC Cardiovasc Imaging 2011;4:1253–1261. doi: 10.1016/j.jcmg.2011.06.023.

7. Judd RM, Reeder SB, Atalar E, McVeigh ER, Zerhouni EA. A Magnetization-Driven Gradient Echo Pulse Sequence for the Study of Myocardial Perfusion. Magn Reson Med 1995;34:276–282.

8. Kim D, Cernicanu A, Axel L. B0 andB1-insensitive uniformT1-weighting for quantitative, first-pass myocardial perfusion magnetic resonance imaging. Magn Reson Med 2005;54:1423–1429. doi: 10.1002/mrm.20704.

9. Jerosch-Herold M, Wilke N, Stillman AE. Magnetic Resonance Quantification of the Myocardial Perfusion Reserve With a Fermi Function Model for Constrained Deconvolution. Medical Physics 1998;25:73–84.

10. Cernicanu A, Axel L. Theory-Based Signal Calibration with Single-Point T1 Measurements for First-Pass Quantitative Perfusion MRI Studies. Acad Radiol 2006;13:686–693. doi: 10.1016/j.acra.2006.02.040.

11. Hsu L, Rhoads K, Holly J, Kellman P, Aletras A, Arai A. Quantitative Myocardial Perfusion Analysis With a Dual-Bolus Contrast-Enhanced First-Pass MRI Technique in Humans. J Magn Reson Imaging 2006;23:315.

12. Gatehouse PD, Elkington AG, Ablitt NA, Yang G-Z, Pennell DJ, Firmin DN. Accurate assessment of the arterial input function during high-dose myocardial perfusion cardiovascular magnetic resonance. J Magn Reson Imaging 2004;20:39–45. doi: 10.1002/jmri.20054.

13. Kellman P, Arai AE. Imaging Sequences for First Pass Perfusion - A Review. J Cardiovasc Magn Reson 2007;9:525–537. doi: 10.1080/10976640601187604.

14. Shin T, Hu HH, Pohost GM, Nayak KS. Three dimensional first-pass myocardial perfusion imaging at 3T: feasibility study. J Cardiovasc Magn Reson 2008;10:57. doi: 10.1186/1532-429X-10-57.

15. Tsao J, Kozerke S. MRI temporal acceleration techniques. J Magn Reson Imaging 2012;36:543–560. doi: 10.1002/jmri.23640.

16. Vitanis V, Manka R, Boesiger P, Kozerke S. Accelerated cardiac perfusion imaging using k-t SENSE with SENSE training. Magn Reson Med 2009;62:955–965. doi: 10.1002/mrm.22078.

17. Tsao J, Boesiger P, Pruessmann KP. k-t BLAST and k-t SENSE: Dynamic MRI with High Frame Rate Exploiting Spatiotemporal Correlations. Magn Reson Med 2003;50:1031–1042. doi: 10.1002/mrm.10611.

18. Pedersen H, Kozerke S, Ringgaard S, Nehrke K, Kim WY. k-t PCA: temporally constrained k-t BLAST reconstruction using principal component analysis. Magn Reson Med 2009;62:706–716. doi: 10.1002/mrm.22052.

19. Lustig M, Donoho D, Pauly JM. Sparse MRI: The application of compressed sensing for rapid MR imaging. Magn Reson Med 2007;58:1182–1195. doi: 10.1002/(ISSN)1522-2594.

20. Adluru G, Whitaker R, DiBella E. Spatio-temporal constrained reconstruction of sparse dynamic contrast enhanced radial MRI data. 4th IEEE International Symposium on Biomedical Imaging: From Nano to Macro, 2007. ISBI 2007 2007:109–112.

21. Manka R, Kuhn FP, Kuest SM, Gaemperli O, Kozerke S, Kaufmann PA. Hybrid cardiac magnetic resonance/computed tomographic imaging: first fusion of three-dimensional magnetic resonance perfusion and low-dose coronary computed tomographic angiography. European Heart Journal 2011;32:2625. doi: 10.1093/eurheartj/ehr312.

22. Plein S, Ryf S, Schwitter J, Radjenovic A, Boesiger P, Kozerke S. Dynamic contrast-enhanced myocardial perfusion MRI accelerated with k-t sense. Magn Reson Med 2007;58:777–785. doi: 10.1002/mrm.21381.

23. Manka R, Jahnke C, Kozerke S, Vitanis V, Crelier G, Gebker R, Schnackenburg B, Boesiger P, Fleck E, Paetsch I. Dynamic 3-Dimensional Stress Cardiac Magnetic Resonance Perfusion Imaging. Journal of the American College of Cardiology 2011;57:437–444. doi: 10.1016/j.jacc.2010.05.067.

24. Jogiya RR, Kozerke SS, Morton GG, De Silva KK, Redwood SS, Perera DD, Nagel EE, Plein SS. Validation of dynamic 3-dimensional whole heart magnetic resonance myocardial perfusion imaging against fractional flow reserve for the detection of significant coronary artery disease. Journal of the American College of Cardiology 2012;60:756–765. doi: 10.1016/j.jacc.2012.02.075.

25. Motwani M, Jogiya R, Kozerke S, Greenwood JP, Plein S. Advanced Cardiovascular Magnetic Resonance Myocardial Perfusion Imaging: High-Spatial Resolution Versus 3-Dimensional Whole-Heart Coverage. Circulation: Cardiovascular Imaging 2013;6:339–348. doi: 10.1161/CIRCIMAGING.112.000193.

26. Otazo R, Kim D, Axel L, Sodickson DK. Combination of compressed sensing and parallel imaging for highly accelerated first-pass cardiac perfusion MRI. Magn Reson Med 2010;64:767–776. doi: 10.1002/mrm.22463.

27. Lingala SG, Hu Y, DiBella E, Jacob M. Accelerated dynamic MRI exploiting sparsity and low-rank structure: k-t SLR. IEEE Transactions on Medical Imaging 2011;30:1042–1054. doi: 10.1109/TMI.2010.2100850.

28. Shin T, Nayak KS, Santos JM, Nishimura DG, Hu BS, McConnell MV. Three-dimensional first-pass myocardial perfusion MRI using a stack-of-spirals acquisition. Magn Reson Med 2012:n/a–n/a. doi: 10.1002/mrm.24303.

29. Akçakaya M, Basha TA, Pflugi S, Foppa M, Kissinger KV, Hauser TH, Nezafat R. Localized spatio-temporal constraints for accelerated CMR perfusion. Magn Reson Med 2013:n/a–n/a. doi: 10.1002/mrm.24963.

30. DiBella EVR, Chen L, Schabel MC, Adluru G, McGann CJ. Myocardial perfusion acquisition without magnetization preparation

or gating. Magn Reson Med 2011;67:n/a–n/a. doi: 10.1002/mrm.23318.

31. Giri S, Xue H, Maiseyeu A, Kroeker R, Rajagopalan S, White RD, Zuehlsdorff S, Raman SV, Simonetti OP. Steady-state first-pass perfusion (SSFPP): A new approach to 3D first-pass myocardial perfusion imaging. Magn Reson Med 2013:n/a–n/a. doi: 10.1002/mrm.24638.

32. Jerosch-Herold M. Quantification of myocardial perfusion by cardiovascular magnetic resonance. J Cardiovasc Magn Reson 2010;12:57. doi: 10.1186/1532-429X-12-57.